Measurement of Station Delay at DSS-25

Dustin Buccino,* Jim Border,† Christopher Volk,† and Oscar Yang*

ABSTRACT. — This article discusses a measurement of the station delay at the Deep Space Network's DSS-25 antenna in support of the Juno Gravity Science investigation. Calibration of the station delays in radiometric measurements is crucial in the computation of spacecraft trajectories and gravitational fields. Due to the high dynamics experienced by the Juno spacecraft, the accuracy of the Doppler measurements is more sensitive to small errors in the calibration. To support the Juno Gravity Science investigation, a test was conducted in November 2018 to measure the phase delay from the transmitter to the DSS-25 antenna and back to the receivers along three signal paths: X-up/X-down, X-up/Ka-down, and Ka-up/Ka-down. Both the uplink signal generation equipment and the receiver equipment are located at the Goldstone Signal Processing Center, approximately 10 kilometers direct line-of-sight away from the DSS-25 antenna. The previous estimate of the station delay at DSS-25 is 77 microseconds one-way (154 microseconds round-trip). Here we present results that the measured round-trip X-up/X-down and X-up/Ka-down delay is fairly close to the previous estimate with a delay of 151 microseconds, but the Ka-up/Ka-down delay is 24 microseconds longer and is attributable to the Ka-band uplink. We recommend new values to be used for station delay at DSS-25.

I. Introduction

The Juno Radio Science investigation utilizes coherent (two-way) frequency observables at X-band and Ka-band to improve the gravitational field model of Jupiter. The primary frequency observables are derived from open-loop recordings of Juno's perijove (closest-approach) passes of Jupiter. By design, these passes occur over DSS-25 in order to use the Ka-band transmitter for dual X-up/X-down and Ka-up/Ka-down measurements. The Juno spacecraft at Jupiter is in a highly elliptical, polar orbit coming within 4000 km of the cloud tops of the planet. Juno measures the gravitational field of the planet during perijove based on the received Doppler frequency observables at X-band and Ka-band. Due to Jupiter's massive size, the radio link undergoes extremes in Doppler dynamics, up to 6.25 MHz at Ka-band during perijove [1].

* Communications Architectures and Research Section.

† Tracking Systems and Applications Section.

The research described in this publication was carried out by the Jet Propulsion Laboratory, California Institute of Technology, under a contract with the National Aeronautics and Space Administration.

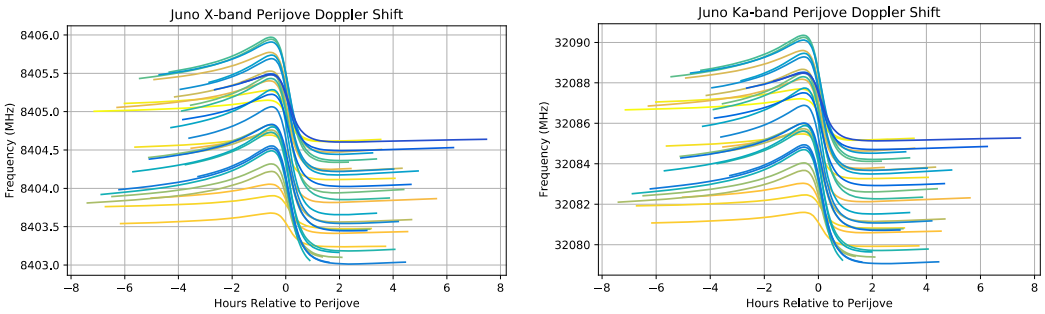

Figure 1. Juno Doppler profiles during perijove, with X-band on the left (a) and Ka-band on the right (b). Each line represents a different perijove.

With these high dynamics, it is critical to understand the station delay. The current best estimate of the one-way station delay at DSS-25 is 77 microseconds (applied twice: once at the uplink time and once at the downlink time).

This paper discusses the measurements done on 2018 DOY 333 to measure the delay at DSS-25 using the ramped ranging technique. First, the methodology and delay measurement equations are described. Second, the test setup is discussed. Next, the results of the delay test are discussed. The paper concludes with recommendations based on these results how to implement the new delays within the Juno Gravity Science team.

II. Methodology

In the most basic sense, a range measurement is simply the time delay between a transmitted signal and received signal. For a direct measurement of the carrier delay, the ramped ranging technique is used. The ramped ranging technique works by measuring the time shift on a signal whose frequency is changed as a function of time by a constant value (the slope, referred to as the "ramp"):

$$f_{TX}\left(t\right) = f_{TX,0} + \dot{f}_{TX}\left(t - t_0\right) \tag{1}$$

Where f_0 is the initial frequency in Hz, $\dot{f}$ is the ramp rate in Hz/second, t is time in seconds, and t_0 is the time the frequency begins to ramp. The subscript TX indicates it is the transmitted frequency profile and subscript RX indicates it is the received frequency profile. If there was no delay, the received frequency profile would then be the transmitted profile multiplied by the turnaround ratio TAR:

$$f_{RX,pred}\left(t\right) = f_{TX}\left(t\right) * TAR \tag{2}$$

However, the actual received frequency is time shifted by the delay d before being multiplied by the turnaround ratio:

$$f_{RX,obs}\left(t\right) = f_{TX}\left(t + d\right) * TAR \tag{3}$$

The difference between the observed and predicted is called the frequency residual Δf:

$$\Delta f = f_{obs} - f_{pred} = \left[f_{TX}(t) - f_{TX}(t+d) \right] * TAR \tag{4}$$

Substituting Equation (1) into Equation (4) and simplifying yields the elegant solution:

$$\Delta f = -\left(\dot{f}_{TX} * TAR \right) d \tag{5}$$

Therefore, the delay may be measured by dividing the residual frequency by the ramp rate:

$$d = -\frac{\Delta f}{\dot{f}_{TX} * TAR} \tag{6}$$

Graphically, each test to measure the delay is a piecewise linear function with three segments: (1) an inbound baseline where the frequency is held fixed at the initial frequency value; (2) the ramped portion where the frequency changes linearly as a function of time; and (3) an outbound baseline where the frequency is held fixed at the final frequency value. This is displayed in Figure 2.

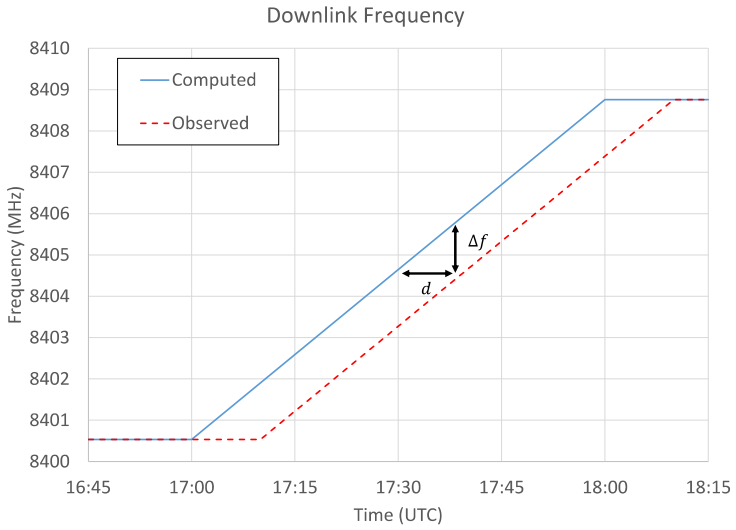

Figure 2. An exaggerated graphical representation of the predicted frequency (equal to transmit frequency multiplied by turnaround ratio) and the actual observed frequency.

III. Test Implementation

In order to measure the delay at the station, the uplink exciter (which generates the uplink signal) and downlink receivers (which track and record the downlink frequency) were configured the same as during a normal Juno pass. However, instead of transmitting and receiving with the spacecraft, a test translator was placed at the antenna that converts the uplink signal, just prior to the antenna transmit path, to a downlink signal connected to the downlink path. Test translators keep phase coherency and multiplies the signal by the turnaround ratio.

The configuration of the DSN is shown in Figure 3. The X-band and Ka-band exciters were ramped through the desired uplink frequency ranges. The X-band transmit signal was

piped simultaneously through the X/X test translator and X/Ka test translator. The Ka-band transmit signal was piped through the Ka/Ka test translator. After passing through the test translators, the signals went through the RF-to-IF downconversion and into the IF distribution network. The downlink signal was recorded by the open-loop receivers (Wideband VLBI Science Receiver–WVSR). The expected received P_c/N_0 on the recorders was 50 dB-Hz (but varied due to fluctuations in temperature and frequency in the cables by ±3 dB-Hz).

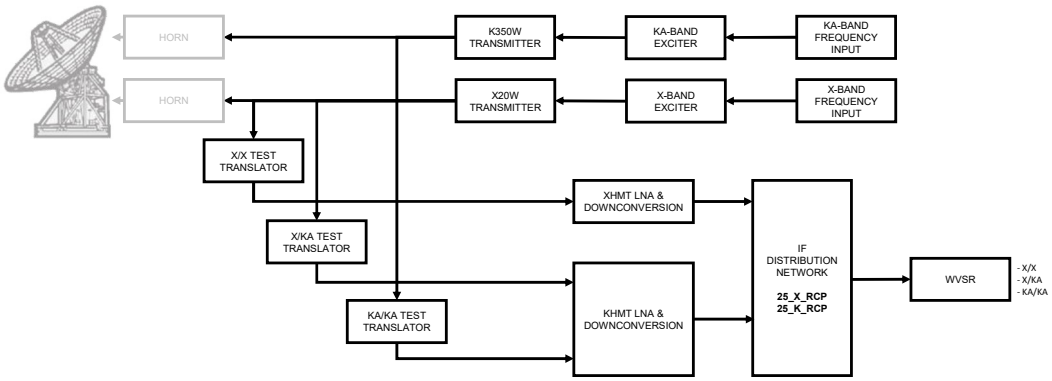

Figure 3. Block-level diagram of the DSN setup to measure the station delay.

Juno's Doppler dynamics are extreme, with one-way Doppler ranges of 1.5 MHz at X-band and 6.25 MHz at Ka-band [1]. The initial Doppler frequency is different for each perijove, and all downlink frequencies range from 8403–8406 MHz at X-band and 32079–32091 MHz at Ka-band, as shown in Figure 1. The expected received downlink frequencies from Juno perijove are multiplied by the respective turnaround ratios [2] to compute the corresponding uplink frequency ranges. An additional few MHz of padding is added on each end for buffer.

With an internally generated signal piped through the test translators, the noise sources are the ground frequency and timing subsystem (FTS), ground electronics, and thermal noise. The expected Doppler accuracy σ_f (1-sigma) may be computed[1] as:

$$\sigma_f = \frac{\sqrt{2B_L}}{2\pi T_c \sqrt{P_c/N_0}} \tag{7}$$

Where B_L is the carrier loop bandwidth, T_c is the count-time of the Doppler measurement, and P_c/N_0 is the signal-to-noise ratio. Optimal open-loop processing places a constraint of $B_L = 1/2T_c$,[1] therefore, Equation (7) can be simplified to:

$$\sigma_f = \frac{1}{2\pi\sqrt{T_c^3}\sqrt{P_c/N_0}} \tag{8}$$

[1] J. Border and W. Folkner, Thermal Noise Contribution to Doppler Measurement Error, JPL Interoffice Memorandum JSB-13-09-08, September 18, 2013.

Thus, with Pc/No of 50 dB-Hz, the Doppler accuracy of a 1-second count time measurement is 23 mHz, 10-second count time measurement is 0.71 mHz, and 60-second count time measurement is 0.05 mHz.

In order to measure nanosecond-level variations in the station delay with the ramped ranging technique, a tuning rate of 100 kHz/sec is desired, giving an estimated 0.5 ns delay timing precision (with a count time of 60 seconds). For a finer sampling of the frequency variations, the desired tuning rate is set to a slower 5 kHz/sec, giving an estimated 10 ns delay timing precision.

Table 1 gives the specifics on the frequency ranges and tuning rates used during this test. Selection was based on the above constraints from Juno's telecom configuration, expected Doppler dynamics during perijoves, and anticipated accuracy of the Doppler measurement.

Table 1. Specifics of each test to measure delay with ramped ranging.

Configurations	Uplink Frequency Range	TAR	Downlink Frequency Range	Uplink Tuning Rate	Test Duration
X-up/X-down	7150–7157 MHz	880/749	8400.534–8408.758 MHz	5 kHz/sec	1400 sec
				100 kHz/sec	70 sec
X-up/Ka-down	7150–7157 MHz	3360/749	32074.77–32106.17 MHz	5 kHz/sec	1400 sec
				100 kHz/sec	70 sec
Ka-up/Ka-down	34358–34376 MHz	3360/3599	32076.38–32093.18 MHz	5 kHz/sec	3600 sec
				100 kHz/sec	180 sec

Each test was performed twice to provide a backup test in the event the first one was unsuccessful. All tests were successful, so the second test provided a validation of the previous test.

IV. Results

Four tests, two at 5 kHz/sec uplink ramp rate and two at 100 kHz/sec uplink ramp rate were successfully completed for each configuration (X/X, X/Ka, and Ka/Ka), for a total of 12 datasets. The signal was recorded open-loop on the Wideband VLBI Science Receiver (WVSR). The WVSR records the in-phase and quadrature (IQ) samples with a 1-kHz recording bandwidth around the predicted frequency.

To estimate frequency from the IQ data, a second-order phase-locked loop (PLL) was used which provided frequency estimates every second. The frequency estimates were then converted up to sky frequency level, which were the Doppler observables. The Doppler observables were then compressed to 10-second count time and 60-second count time by integrating to phase and fitting a line to 10 and 60 data points, respectively, where the slope of the linear fit was the frequency at the midpoint. This data processing is the same method used for the Juno Gravity Science investigation [3].

The average Doppler noise is summarized in Table 2. The noise is comparable to the predicted values from thermal noise theory [4], but differs due to fluctuations in P_c/N_0 during the testing.

Table 2. Average Doppler noise across all tests during the baseline (non-ramped at a fixed frequency).

Configuration	Receiver	IFS	1 s Doppler Noise (Hz)	10 s Doppler Noise (Hz)	60 s Doppler Noise (Hz)
X-up/X-down	WVSR2B	25_X_RCP	4.8E-04	7.5E-05	1.8E-05
X-up/Ka-down	WVSR2A	25_K_RCP	9.0E-04	1.4E-04	2.2E-05
Ka-up/Ka-down	WVSR2A	25_K_RCP	9.0E-04	1.1E-04	1.9E-05
Predicted			*2E-02*	*7E-04*	*5E-05*

The frequency residuals were computed from the Doppler observables by subtracting the predicted frequency, described by Equations (2), (3), and (4). A 60-second count time was used for Tests #1 and #2, and a 10-second count time was used for Tests #3 and #4. The delay was then computed from the frequency residuals using Equation (6), and plotted against the uplink frequency. A linear fit was done on the delay as a function of uplink frequency in order to determine if there was any frequency dependence on the delay. For X-up/X-down, the delay caused by the test translator was approximately 20 nanoseconds and was removed to produce a calibrated round-trip delay estimate. The delay on the X-up/Ka-down and Ka-up/Ka-down test translators was not measured but is expected to be about the same order of magnitude. Future plans are in place to measure the instrumental delay in the X-up/Ka-down and Ka-up/Ka-down test translators. Figure 4, Figure 5, and Figure 6 show an analysis of this step by step: first, showing the observed and computed frequencies; second, showing the frequency residuals (the difference between computed and observed values); and third, showing the computed delays from the frequency residuals.

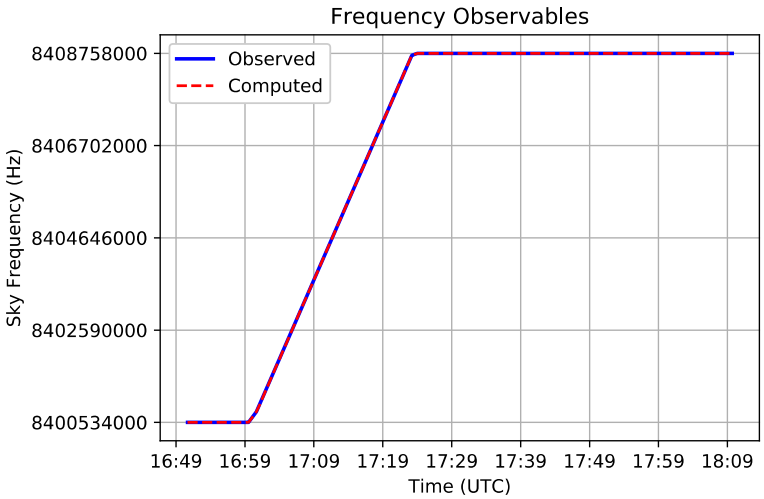

Figure 4. Frequency observables from Test #1 in the X-up/X-down configuration. The ramp at 2.5 kHz/second begins at 17:00:00 UTC and ends at 17:23:20 UTC.

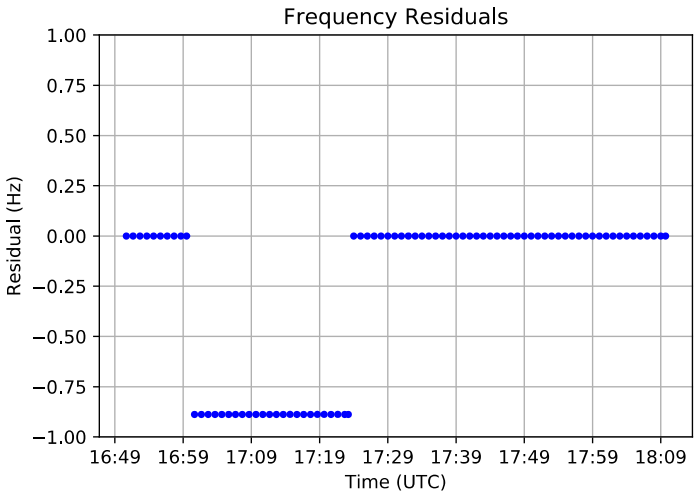

Figure 5. Frequency residuals from Test #1 in the X-up/X-down configuration. During the period of ramping beginning at 17:00 UTC, a non-zero residual frequency is observed, indicating the delay between transmission and reception.

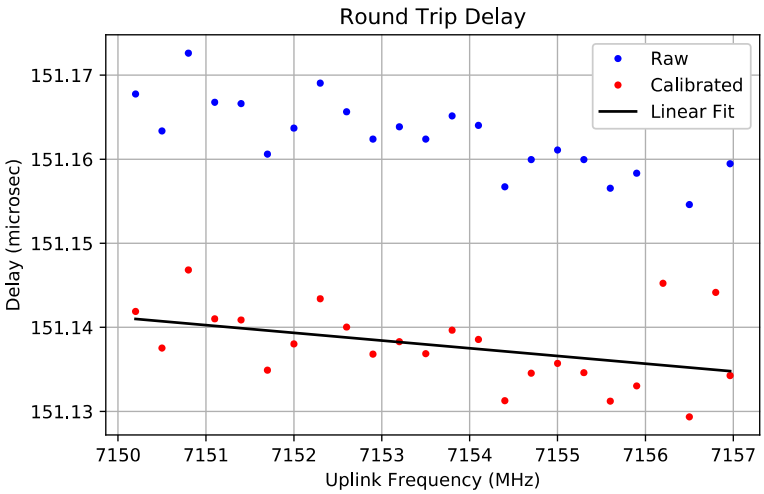

Figure 6. Results of the station delay as a function of the instantaneous uplink frequency from Test #1 in the X-up/X-down configuration. The raw observables (blue) are calibrated to remove the test transponder delay (red). A small linear dependence is present across the uplink frequency band.

Tests #2, #3, and #4 are analyzed similarly. The results from each test are summarized in Table 3. The first column is the test number and second column is the mean estimated round-trip delay. The third column is the mean one-way delay, which is simply the round-trip delay divided by two. The uncertainties on each measurement are the standard deviation of the measurement minus the mean. For Tests #1 and #2, the 60-second Doppler count time was used. For Tests #3 and #4, the 10-second Doppler count time was used. The final four columns display the parameters from the polynomial fit, which is described as:

$$d = p_1\left(f_{ul} - f_{ul,0}\right) + p_0 \tag{9}$$

where p_1 and p_0 are the delay coefficients (columns 4 and 5), f_{ul} is the uplink frequency in megahertz, and $f_{ul,0}$ is an arbitrary frequency offset (7150 MHz for X-band uplink and 34357 MHz for Ka-band uplink). Column 6 is the standard error of the linear fit. The final column gives the maximum deviation of the linear fit across the test bandwidth.

Table 3. Summary of results from each individual test.

Configuration	Mean Round-Trip Delay	Mean One-Way Delay	Round-Trip Delay Linear Fit Coefficients $d = p_1\left(f_{ul} - f_{ul,0}\right) + p_0$			
	(µs)	(µs)	p_1 (µs/MHz)	p_0 (µs)	σ (µs)	$\lvert t_f - t_0 \rvert$ (µs)
X-up/X-down						
Test #1	151.13 ± 0.01	75.569 ± 0.007	-9.184E-04	151.131	0.004	0.006
Test #2	151.14 ± 0.01	75.571 ± 0.006	-8.150E-04	151.144	0.004	0.005
Test #3	151.140 ± 0.007	75.570 ± 0.003	-1.247E-03	151.145	0.0009	0.006
Test #4	151.141 ± 0.004	75.570 ± 0.002	-5.210E-04	151.143	0.0009	0.003
X-up/Ka-down						
Test #1	151.10 ± 0.01	75.548 ± 0.007	-1.322E-04	151.097	0.004	0.009
Test #2	151.10 ± 0.004	75.550 ± 0.002	-5.433E-05	151.010	0.002	0.0004
Test #3	151.099 ± 0.002	75.546 ± 0.001	5.757E-05	151.100	0.0006	0.0002
Test #4	151.099 ± 0.002	75.549 ± 0.001	-2.169E-04	151.100	0.0006	0.001
Ka-up/Ka-down						
Test #1	175.06 ± 0.04	87.52 ± 0.02	1.144E-03	175.046	0.01	0.02
Test #2	175.06 ± 0.04	87.53 ± 0.02	1.898E-03	175.044	0.006	0.03
Test #3	175.062 ± 0.009	87.532 ± 0.004	5.004E-04	175.058	0.001	0.008
Test #4	175.063 ± 0.009	87.532 ± 0.005	5.678E-04	175.057	0.002	0.009

Several conclusions may be drawn from the results. For X-up/X-down configuration, the mean round-trip delay is approximately 151 microseconds and has a clear linear change with frequency. This is also seen clearly in Figure 7, where all the delay measurements are plotted as a function of uplink frequency. For X-up/Ka-down, the delay is approximately the same as the X-up/X-down at about 151 microseconds. Unlike X-up/X-down, there is not a conclusive dependence on frequency and the delay remains relatively flat, which is evident in Figure 8. For Ka-up/Ka-down, the delay is significantly larger than the other configurations, with a mean one-way delay of approximately 175 microseconds. A linear trend is detectable, changing the delay a few nanoseconds over the bandwidth. This trend can also been seen in Figure 9.

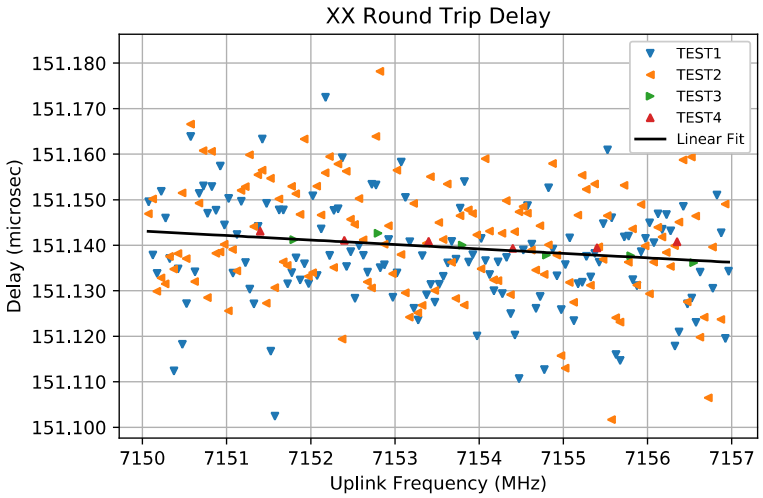

Figure 7. X-up/X-down delay as function of uplink frequency from all tests.

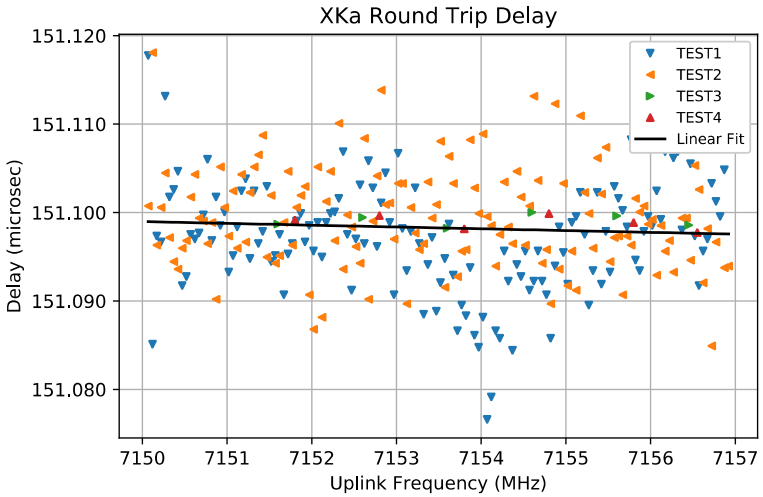

Figure 8. X-up/Ka-down delay as function of uplink frequency from all tests.

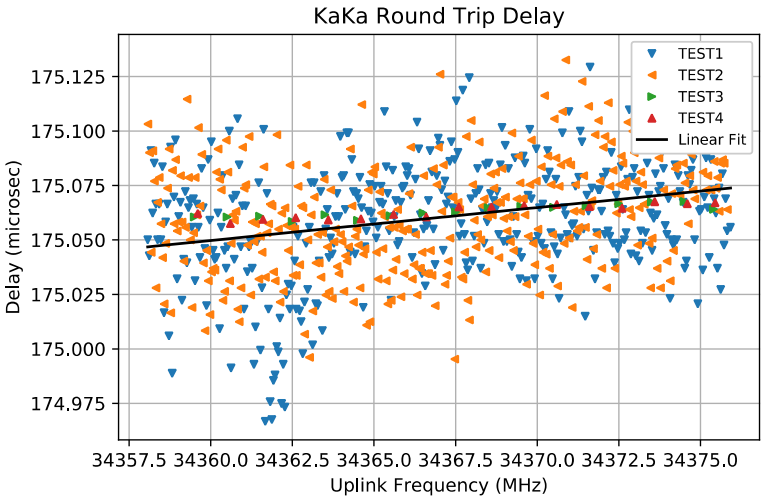

Figure 9. Ka-up/Ka-down delay as function of frequency from all tests.

V. Discussion and Recommendations

The X-up/X-down and X-up/Ka-down have near-identical delays. These configurations share the same uplink path, but a different downlink path. In comparison, the X-up/Ka-down and Ka-up/Ka-down share the same downlink path, but a different uplink path – yet these differ in measured delays by 24 microseconds. Because of the shared signal pathways, it is reasonable to conclude that the 24 microseconds delay bias between the X-up and Ka-up configurations lies entirely in the Ka-band uplink path.

Thus, the average estimated round-trip delay was divided by two in order to get a one-way delay for X-up/X-down and X-up/Ka-down and was assumed to be split equally between the uplink and downlink paths. (It is not possible to separate the uplink and downlink effects for these configurations with this testing alone.) For the Ka-up/Ka-down, the X-up/Ka-down downlink delays are assumed to be equal. Ka-up/Ka-down uplink delay is the difference between the assumed downlink delay and the measured round-trip delay, placing the difference entirely on the Ka-uplink path as concluded above. The delay values are shown in Table 4 are recommended for use.

Table 4. Average measured station delays at DSS-25. These are the values recommended for use.

Configuration	Average Uplink Delay	Average Downlink Delay	Round Trip Delay	Formal Round-Trip Uncertainty	Time Code Translator Accuracy	Round-Trip Linear Delay Variation
	(μs)	(μs)	(μs)	(μs)	(μs)	(μs)
X-up/X-down	75.57	75.57	151.14	0.02	1.0	0.006
X-up/Ka-down	75.55	75.55	151.10	0.03	1.0	N/A
Ka-up/Ka-down	99.51	75.55	175.06	0.08	1.0	0.027

The formal uncertainties are propagated from the individual test results into an average. The X-up/Ka-down and Ka-up/Ka-down uncertainties are increased by 20 ns to account for an uncalibrated test translator delay. It is desirable to measure the delay from the X/Ka and Ka/Ka test translators in the future; however, the expected impact on the measurements will be small.

Although the formal round-trip uncertainties are on the order of ~20 ns, it is important to keep in mind the time-tag measurement at each receiver depends on the timestamp *as kept by the receiver.* The DSN's Time Code Translator (TCT) provides time-tags accurate to 1 microsecond at each receiver (810-005, Module 209C, Table 4) [5]. Thus, differences between receivers are possible at the 1-microsecond level. (Note the *time rate* of each receiver uses the same reference frequency.) The time stamp error is not random, but is stable once the receiver and TCT are in sync.

The linear delay variation is the difference between the maximum and minimum values of a polynomial fit to each dataset. As expected, based on the results from the individual tests, for X-up/X-down and Ka-up/Ka-down, the linear delay variation is larger than the formal uncertainty (Table 3). For X-up/Ka-down, there is no detectable variation as a function of frequency.

VI. Conclusion

The round-trip delay at DSS-25 was measured using each band configuration available for use by the Juno mission: X-up/X-down, X-up/Ka-down and Ka-up/Ka-down. The average round-trip X-up/X-down delay was measured to be 151.14 microseconds. The X-up/Ka-down delay was measured to 151.10 microseconds, very similar to X-up/X-down. Surprisingly, the round-trip Ka-up/Ka-down delay was measured to be much higher at 175.06 microseconds – approximately 24 microseconds higher than the other two configurations. Because both X-band uplink configurations have similar delays, and the configuration with Ka-uplink is significantly higher, a reasonable explanation is that this delay is introduced by the Ka-band uplink systems. Thus, the 24 microsecond likely lies entirely on the Ka-band uplink path and we recommend the delay difference be applied on the Ka-uplink only. The physical reason behind the 24 microsecond delay on the Ka-band uplink is currently unknown and is under investigation.

Acknowledgments

The authors would like to thank Albert Kern (DSN Uplink Operations Engineer), Dong Shin (JPL Deep Space Tracking Systems Group), Von Petrovich and Scott Riley (Juno DSN Network Operations team), William Folkner (Juno Lead Gravity Science Co-Investigator), and Kamal Oudrhiri (Planetary Radar and Radio Science Group Supervisor) for their help in supporting this test.

References

[1] D. R. Buccino, D. S. Kahan, O. Yang and K. Oudrhiri, "Extraction of Doppler observables from open-loop recordings for the Juno radio science investigation," 2018 United States National Committee of URSI National Radio Science Meeting (USNC-URSI NRSM), Boulder, CO, 2018a, pp. 1–2.

[2] R. Mukai, D. Hansen, A. Mittskus, J. Taylor, M. Danos, and A. Kwok, "Juno Telecommunications," Vol. 16, Rev. A, Pasadena: Jet Propulsion Laboratory, 2017. *DESCANSO Design and Performance Summary Series.*

[3] D. Buccino, D. Kahan, O. Yang, and K. Oudrhiri, "Initial Operations Experience and Results from the Juno Gravity Experiment," 2018 IEEE Aerospace Conference, Big Sky, MT, 2018, pp. 1–8.

[4] P. H. Phipps, P. Withers, D. R. Buccino, Y.-M. Yang. "Distribution of Plasma in the Io Plasma Torus as Seen by Radio Occultation During Juno Perijove 1," *Journal of Geophysical Research: Space Physics,* Vol 123(8), July 1, 2018.

[5] *DSN Telecommunications Link Design Handbook,* DSN No. 810-005, Rev. F, Jet Propulsion Laboratory, Pasadena, CA. http://deepspace.jpl.nasa.gov/dsndocs/810-005/ .